Detecting phase synchronization in noisy data from coupled chaotic oscillators

Junfeng Sun,* Jie Zhang, Jin Zhou, Xiaoke Xu, and Michael Small
Department of Electronic and Information Engineering, Hong Kong Polytechnic University, Kowloon, Hong Kong, China
(Received 6 November 2007; published 17 April 2008)

Two schemes are proposed to detect phase synchronization from chaotic data contaminated by noise. The first is a neighborhood-based method which links time delay embedding with instantaneous phase estimation. The second adopts the local projection method as a preprocessing filter to noisy data. Both schemes utilize the state recurrence, an important feature of chaotic data. The proposed schemes are applied to data measured from two typical chaotic systems, i.e., the coupled Rössler systems and the coupled Lorenz systems, respectively. The results show that phase synchronization, which may be buried by noise, is detected even when the noise level is high. Moreover, the overestimation of the degree of phase synchronization, which may be introduced by the Hilbert transform combined with a traditional linear bandpass filter, can be avoided when the data are contaminated by only measurement noise.

DOI: 10.1103/PhysRevE.77.046213 PACS number(s): 05.45.Xt, 05.45.Pq, 05.40.Ca

I. INTRODUCTION

Synchronization, a ubiquitous phenomenon in both natural and engineering systems, has been studied extensively in the past years for its numerous applications in various fields (for a review, cf. [1]). Phase synchronization, as a weak form of synchronization, has been observed in various systems, such as coupled chaotic oscillators [2,3], chaotic laser array [4], biomedical signals [5], and neuronal oscillations [6,7]. Various phase definitions have been introduced. One class of them is based on particular transforms, such as the Hilbert transform [2], the wavelet transform [8], and a generalized transform with a Gaussian filter [4], to the measured data. Another class of phases is defined as the angle of evolving trajectory, which is reconstructed from the two-dimensional projection of the system [1,9] or the time derivative of the projection [3,10], around a fixed point.

For particular data (e.g., data from coherent Rössler systems), an instantaneous phase can be directly obtained with the Hilbert transform [2]. If the data are contaminated by measurement noise, the phase so estimated will involve artificial phase slips, i.e., the discontinuous "jumps" of the unwrapped phase, which do not imply any intrinsic oscillation but are due to noise. For this case, a linear filter with narrow bandwidth is usually first applied to the noisy data, and then phase is estimated from the output of the filter. However, on the one hand, the linear filter with narrow bandwidth may lead to a spurious overestimation of the actual degree of phase synchronization [11]; on the other hand, the linear filter with broad bandwidth will leave a certain amount of intraband noise, and thus cannot suppress the effect of noise effectively. Recently, a data-driven filter has been proposed [12]. It is argued that this filter can reduce the noise-induced susceptibility of the estimated phase.

Some other methods have also been proposed to detect (phase) synchronization in noisy data. For example, surrogate data methods are applied to provide significance tests of phase synchronization in noisy data [13], where both the noisy data and their surrogate data are passed through a linear filter first. However, it is reported that weak synchronization may be artificially detected even from two independent and identically distributed Gaussian noise series after narrow bandwidth filtering [11]. So surrogates also suffer from the effect of linear filtering and should be used carefully. Nonlinear interdependence is proposed to characterize the degree of generalized synchronization, utilizing the mutual neighbors and the feature that similar initials lead to similar successors in the evolving chaotic system [14–16]. The performances of various synchronization measures, including nonlinear interdependence, mutual information, and phase based on both the Hilbert transform and wavelet transform, are compared with real electroencephalographic (EEG) data. It shows that these measures can indicate a similar tendency in the degree of synchronization [17]. Further, these measures are tested with data (from typical coupled chaotic systems) which are contaminated by measurement noise. Results show that these measures work effectively when the noise level is low, but can be greatly degraded when the noise level is relatively high [18]. It is difficult to say which measure is the best in general. Recently, a statistical measure of recurrences is proposed to detect phase synchronization, and is robust for measurement noise [3]. After that, a general framework is proposed to detect phase synchronization through localized sets rather than defining the instantaneous phase straightforward [19]. This framework can be applied to oscillators with multiple time scale (e.g., spiking and/or bursting neurons). However, whether it is robust to noise or not is (as far as we are aware) not reported yet. Moreover, these two methods can only quantify the degree of synchronization in the mean.

To overcome the limitations discussed above, two schemes are proposed to estimate the instantaneous phase for noisy chaotic data from the viewpoint of time delay embedding. State recurrence, an important feature of chaotic systems, is utilized. In phase space reconstructed by time delay embedding [20], the state recurrences of a reference vector turn out to be its nearest neighbors. These neighbors can provide redundant information [21] and have been successfully utilized in chaotic time series analysis and processing, such as prediction [22], time-frequency analysis [21], detec-

*sun.junfeng@polyu.edu.hk

tion of state transitions [23], and noise reduction (the local projection method) [24–29].

The first scheme is a neighborhood-based phase estimation (NPE) method. The reference vector and its nearest neighbors (i.e., state recurrences) cover segments of data with a similar wave form [21]. This implies that the analytical trajectories (constructed with the Hilbert transform [2]) corresponding to the reference vector and its neighbors are close to each other in the Hilbert plane, as will be illustrated later. With this observation, the instantaneous phase of noisy data is estimated by a certain averaging of the corresponding instantaneous phase of the neighbors. The second scheme uses the local projection (LP) method, instead of the traditional linear bandpass filter, as a preprocessing filter to noisy data. Then the instantaneous phase can be obtained with the Hilbert transform after noise reduction. Simulation results show that the instantaneous phase estimated by both proposed schemes suffers much less from the artificial phase slips, and thus phase synchronization (both in local time and in whole time), which may otherwise be buried by measurement noise, is successfully detected.

The organization of this paper is as follows. In Sec. II, the relationship between the nearest neighbors and their corresponding analytical trajectories is demonstrated, and then the principle of NPE is proposed. Further, the LP method is briefly reviewed. In Sec. III, the proposed schemes are applied to data measured from both coupled Rössler systems and coupled Lorenz systems, respectively. Finally, conclusions and discussions are given in Sec. IV.

II. PRINCIPLE OF THE METHODS

A. Neighborhood-based phase estimation

The most popular definition of instantaneous phase is based on the Hilbert transform. The analytic signal of $s(t)$ is defined as

$$s^{(a)}(t) = s(t) + j\tilde{s}(t) = A(t)e^{j\phi(t)}, \tag{1}$$

where $\tilde{s}(t)$ is the Hilbert transform of $s(t)$,

$$\tilde{s}(t) = \frac{1}{\pi}\mathrm{P}\int_{-\infty}^{\infty}\frac{s(\nu)}{t-\nu}d\nu \tag{2}$$

(here P means that the integral is taken in the sense of Cauchy principal value). Then the instantaneous phase of signal $s(t)$ is

$$\phi(t) = \arctan\frac{\tilde{s}(t)}{s(t)}. \tag{3}$$

To illustrate the method of neighborhood-based phase estimation (NPE), the following coupled nonidentical Rössler systems [5] are taken as an example:

$$\dot{x}_{1,2} = -\omega_{1,2}y_{1,2} - z_{1,2} + \zeta_{1,2} + \varepsilon(x_{2,1} - x_{1,2}),$$

$$\dot{y}_{1,2} = \omega_{1,2}x_{1,2} + \alpha y_{1,2},$$

$$\dot{z}_{1,2} = \beta + z_{1,2}(x_{1,2} - \gamma), \tag{4}$$

where $\omega_{1,2}=1\pm0.015$, ε is the coupling strength, $\zeta_{1,2}\sim N(0,\sigma_\zeta^2)$, and σ_ζ is the standard deviation of the dynamic noise. Data are integrated from variables $x_{1,2}$ using the fourth-order Runge-Kutta method (Matlab function *ode45*) with sampling interval $\Delta t=0.2$. The initial values are set randomly, and 10 000 samples are adopted after the transient state. The measured time series is denoted as $s_{1,2}(n\Delta t)=x_{1,2}(n\Delta t)+\xi_{1,2}(n\Delta t)$, where $\xi_{1,2}$ is measurement noise, and assumed to be Gaussian white noise $\xi_{1,2}\sim N(0,\sigma_{\xi_{1,2}}^2)$. To simplify notation, Δt is omitted and $s_{1,2}(n\Delta t)$ is written as $s_{1,2}(n)$ from now on.

Given the time series $\{s(n)\}_{n=1}^{L}$ with $L=10\,000$ samples, the time delay vectors can be reconstructed by time delay embedding [20], i.e., $\{\mathbf{s}(n)\}_{n=1+(d-1)\tau}^{L}$,

$$\mathbf{s}(n) = [s(n-(d-1)\tau), s(n-(d-2)\tau), \ldots, s(n-\tau), s(n)]^{\mathrm{T}},$$

where d is embedding dimension, τ is an integer number which is use to indicate the amount of time delay (i.e., $\tau\Delta t$), and $(\cdot)^{\mathrm{T}}$ denotes the transpose of a real matrix. The neighborhood of the reference vector $\mathbf{s}(n)$ is defined as

$$\mathbf{N}(n) \triangleq \{\mathbf{s}(k):\|\mathbf{s}(k)-\mathbf{s}(n)\| < r, 1+(d-1)\tau \le k \le L\}, \tag{5}$$

where r is the neighborhood radius. For the measured time series $\{s(n)\}$, its Hilbert transform is denoted as $\{\tilde{s}(n)\}$. Corresponding to time delay vector $(\mathbf{s}(n))$, the time delay vector of $(\tilde{s}(n))$ is $\tilde{\mathbf{s}}(n)=[\tilde{s}(n-(d-1)\tau),\tilde{s}(n-(d-2)\tau),\ldots,\tilde{s}(n-\tau),\tilde{s}(n)]^{\mathrm{T}}$. Note that $\tilde{\mathbf{s}}(n)$ is not calculated from $\mathbf{s}(n)$, but is formed from $\{\tilde{s}(n)\}$ by time delay embedding, and $\{\tilde{s}(n)\}$ is integrated in the whole time domain [Eq. (2)], while $\tilde{\mathbf{s}}(n)$ is mainly contributed by the vicinity of $\mathbf{s}(n)$ in time.

Figure 1 illustrates the relationship between the reference vector and its neighbors in the time domain and in the $(s,\tilde{s})$ plane. It shows that the reference vector and its neighbors cover segments of data with similar wave forms [Fig. 1(a)], and thus their corresponding analytical trajectories of clean data are close to each other [Fig. 1(b)]. However, the related trajectories of noisy data appear irregularly [Fig. 1(c)], which will yield artificial phase slips. To deal with this problem, NPE is proposed as follows.

For reference vector $\mathbf{s}(n)$, the average of its neighbors is

$$\bar{\mathbf{s}}(n) = \frac{1}{N}\sum_{\mathbf{s}(k)\in\mathbf{N}(n)}\mathbf{s}(k), \tag{6}$$

and the average of the related neighbors of $\tilde{\mathbf{s}}(n)$ is

$$\bar{\tilde{\mathbf{s}}}(n) = \frac{1}{N}\sum_{\tilde{\mathbf{s}}(k):\mathbf{s}(k)\in\mathbf{N}(n)}\tilde{\mathbf{s}}(k), \tag{7}$$

where $N=|\mathbf{N}(n)|$ is the number of neighbors. Let $\bar{\mathbf{s}}^{(a)}(n)=\bar{\mathbf{s}}(n)+j\bar{\tilde{\mathbf{s}}}(n)$ denote the estimation of the analytical trajectory of $\mathbf{x}(n)$, and $\mathbf{s}(n;i)$ denote the ith entry of $\mathbf{s}(n)$. Then $\bar{\mathbf{s}}^{(a)}(n;i)$ is an estimation of the analytical signal at instant $[n-(d-i)\tau]\Delta t$. As $s(n)$ appears as an entry of $\mathbf{s}(l), l=n,\ldots,n+(d-1)\tau$, there are d estimations of $\bar{s}^{(a)}(n)$ at instant $n\Delta t$. It is difficult to say which estimation is the best, so

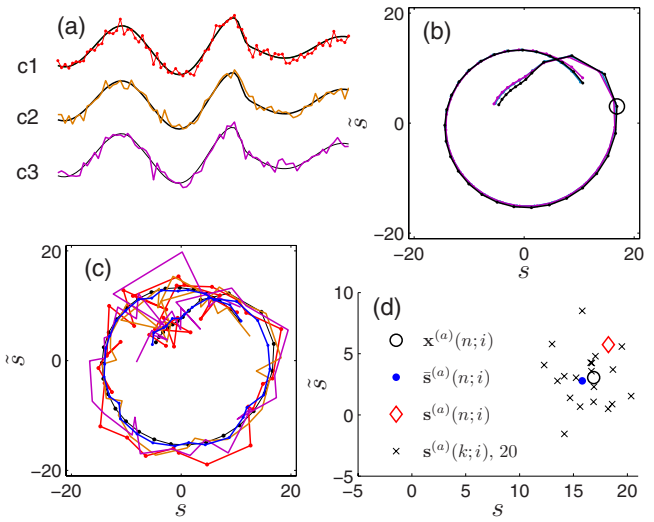

FIG. 1. (Color online) The relationship between the reference vector and its neighbors in the time domain (a) and in the $(s,\tilde{s})$ plane [(b), (c), and (d)]. In this figure, the data are measured from variable x_1 of the coherent Rössler systems [Eq. (4)], with parameters $\varepsilon=0.035$, $\alpha=0.15$, $\beta=0.2$, $\gamma=10$, $\sigma_{\zeta_{1,2}}=0$, $\sigma_{\xi_{1,2}}=0.3\sigma_{x_{1,2}}$, $\tau=1$, and $d=80$. Curve c1 is the segment covered by the reference vector $\mathbf{s}(n)$, and curves c2 and c3 are the segments covered by two neighbors [$\mathbf{s}(k_1)$ and $\mathbf{s}(k_2)$] of the reference vector, respectively. Note that the neighbors are searched from noisy data, and the smooth curves [i.e., $\mathbf{x}(n)$, $\mathbf{x}(k_1)$, and $\mathbf{x}(k_2)$] are the clean versions of the coarse curves, respectively. The analytical trajectories [i.e., $\mathbf{x}^{(a)}(n)$, $\mathbf{x}^{(a)}(k_1)$, and $\mathbf{x}^{(a)}(k_2)$] constructed from clean data are very close to each other (b), while the corresponding trajectories [$\mathbf{s}^{(a)}(n)$, $\mathbf{s}^{(a)}(k_1)$, and $\mathbf{s}^{(a)}(k_2)$] of the noisy version seem pell-mell (c). The blue (dark gray) trajectory in (c), estimated by NPE, is close to the corresponding trajectory [black, in (b)] of clean data. For clarity, only the trajectories corresponding to the mid-half segments of the curves in (a) are plotted in (b) and (c), respectively. A particular entry $\mathbf{s}^{(a)}(n;i)$ ($\diamond$) of $\mathbf{s}^{(a)}(n)$, its clean version $\mathbf{x}^{(a)}(n;i)$ [$\circ$ in (b) and (d)], its 20 noisy neighbors $\mathbf{s}^{(a)}(k;i)$ ($\times$), and the average $\bar{\mathbf{s}}^{(a)}(n;i)$ of these 20 neighbors ($\bullet$) are illustrated in (d).

the average of the estimations at the same instant is taken as the final estimation of the analytical signal at this instant, yielding the estimated analytical signal $\{\bar{\bar{s}}^{(a)}(n)\}$, where $\bar{\bar{s}}^{(a)}(n)=\bar{s}(n)+\bar{\tilde{s}}(n)$. Then the instantaneous phase is estimated as

$$\hat{\phi}(n)=\arctan\frac{\bar{\tilde{s}}(n)}{\bar{s}(n)}. \tag{8}$$

B. Noise reduction by local projection

The local projection (LP) method has been studied extensively [24–29]. Here only the basics of LP are reviewed. The implementation details, extensions, and applications of this method can be found in [26–29] and references therein.

The LP method assumes that the noise is white noise, and thus the local phase space, i.e., the neighborhood $\mathbf{N}(n)$ of the reference point $\mathbf{s}(n)$, can be divided into an M-dimensional *signal subspace* and a $(d-M)$-dimensional *noise subspace*, where M is the minimum embedding dimension of the dynamical system. The signal subspace contains most of the clean signal plus a certain, small, amount of the noise components, while the noise subspace contains most of the noise components. For a preset M, the noise subspace can be estimated by minimizing the total energy that is distributed in it because the energy of white noise is almost uniformly distributed on each direction of the local phase space. The minimization turns out to be the standard eigenvalue decomposition for the covariance matrix $\mathbf{C}(n)$ of the neighborhood $\mathbf{N}(n)$, i.e., $\mathbf{C}(n)\mathbf{u}_i-\lambda_i\mathbf{u}_i=0$, where the matrix $\mathbf{C}(n)$ is defined as $\mathbf{C}(n)=1/N\Sigma_{\mathbf{s}(k)\in\mathbf{N}(n)}[\mathbf{s}(k)-\bar{\mathbf{s}}(n)][\mathbf{s}(k)-\bar{\mathbf{s}}(n)]^{\mathrm{T}}$. Sorting the eigenvalues $\Lambda=\mathrm{diag}(\lambda_1,\lambda_2,\ldots,\lambda_d)$ in descending order, the eigenvectors $\mathbf{U}_1=[\mathbf{u}_1,\ldots,\mathbf{u}_M]$ and $\mathbf{U}_2=[\mathbf{u}_{M+1},\ldots,\mathbf{u}_d]$ span the signal subspace and the noise subspace, respectively, where $\mathbf{u}_i$ is the eigenvector associated with the ith largest eigenvalue. Then the phase vector $\mathbf{s}_n$ can be decomposed as $\mathbf{s}_n=\bar{\mathbf{s}}(n)+\mathbf{U}_1\mathbf{U}_1^{\mathrm{T}}[\mathbf{s}(n)-\bar{\mathbf{s}}(n)]+\mathbf{U}_2\mathbf{U}_2^{\mathrm{T}}[\mathbf{s}(n)-\bar{\mathbf{s}}(n)]$ in the local phase space, where $\mathbf{U}_1\mathbf{U}_1^{\mathrm{T}}[\mathbf{s}(n)-\bar{\mathbf{s}}(n)]$ and $\mathbf{U}_2\mathbf{U}_2^{\mathrm{T}}[\mathbf{s}(n)-\bar{\mathbf{s}}(n)]$ are the projections of $[\mathbf{s}(n)-\bar{\mathbf{s}}(n)]$ in the signal subspace and in the noise subspace, respectively. Eliminating $\mathbf{U}_2\mathbf{U}_2^{\mathrm{T}}[\mathbf{s}(n)-\bar{\mathbf{s}}(n)]$, the enhanced signal vector is obtained,

$$\hat{\mathbf{x}}(n)=\bar{\mathbf{s}}(n)+\mathbf{U}_1\mathbf{U}_1^{\mathrm{T}}[\mathbf{s}(n)-\bar{\mathbf{s}}(n)]. \tag{9}$$

As each element of the time series $\{s(n)\}$ appears as an entry of one of d successive time delay vectors, $\mathbf{s}(l)$, $l=n,\ldots,n+(d-1)\tau$, there are d enhancements of entry $s(n)$ which may be different in value. The arithmetic mean over these values is then taken as the enhanced element $\hat{x}(n)$.

After noise reduction, instantaneous phase can be obtained from $\{\hat{x}(n)\}$ with the Hilbert transform. This scheme just uses the LP method, instead of the traditional linear bandpass filter, as a preprocessing filter to noisy data, and is denoted by P-LP. It has been reported that the LP method is more powerful than the linear bandpass method in reducing noise for chaotic data [24,25,27].

III. SIMULATION RESULTS

A. Phase synchronization of coupled Rössler systems

First, the proposed schemes are applied to data measured from coupled coherent Rössler systems [Eq. (4)] with no dynamic noise. The parameters are set as $\alpha=0.15$, $\beta=0.2$, $\gamma=10$, $\sigma_{\zeta_{1,2}}=0$, and $\sigma_{\xi_{1,2}}=\eta\sigma_{x_{1,2}}$, where η is the level of measurement noise.

Figure 2 illustrates the detection of phase synchronization by the proposed schemes. Let P-HT denote the method that phase is obtained by applying the Hilbert transform directly to (noisy) data. It can be observed that when there is measurement noise, the instantaneous phase difference $(\phi_1-\phi_2)$ of the coupled systems [Eq. (4)], estimated by P-HT, fluctuates irregularly [Fig. 2(a), "P-HT, $\eta=0.5$" and "P-HT, $\eta=0.7$"], and the wrapped phase difference $\Delta\Psi_{1,2}=(\phi_1-\phi_2)\mathrm{mod}(2\pi)$ exhibits a much broader distribution compared with that of the corresponding clean data [Figs. 2(c) and 2(d) vs Fig. 2(b)]. This may mislead that the coupled oscillators are nonsynchronous or weakly synchronous, though the intrinsic oscillations are synchronous [Fig. 2(a),

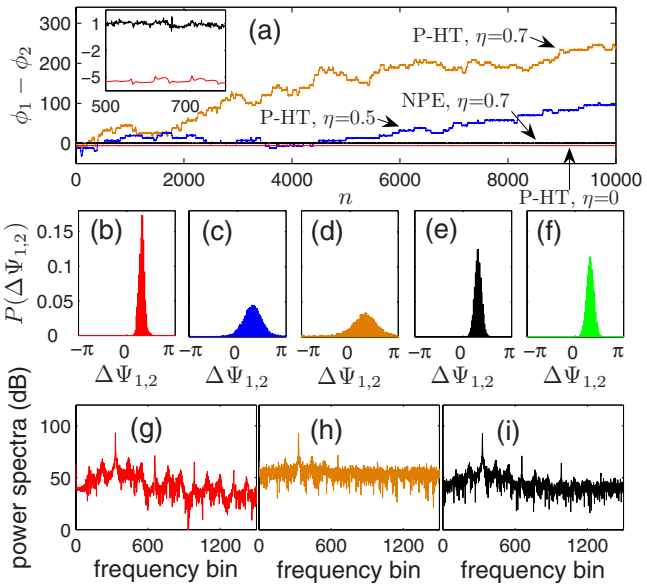

FIG. 2. (Color online) Phase synchronization of synchronous Rössler systems (ε=0.035). (a) The unwrapped phase difference of systems (1, 2). (b)–(d) are the distributions $P(\Delta\Psi_{1,2})$ of the wrapped phase difference of the cases η=0 (i.e., clean), η=0.5, and η=0.7 by P-HT, respectively. (e) and (f) are the results of noisy data (η=0.7) by NPE and P-LP (τ=1, d=80, N=20, and M=5), respectively. (g)–(i) are the power spectra of the clean data, noisy data (η=0.7), and the real part $\{\bar{s}(n)\}$ of the estimated analytical signal $\{\bar{s}^{(a)}(n)\}$ by NPE, respectively. Note that only the low frequency region of the power spectra is plotted. The power spectra of the data after noise reduction by LP are similar to that in (i), and are not plotted.

"P-HT, η=0"]. However, this misclassification can be avoided by NPE and P-LP. The unwrapped phase difference [Fig. 2(a), "NPE η=0.7"] estimated by the proposed schemes is bounded around a constant, indicating phase synchronization, and the corresponding distribution $P(\Delta\Psi_{1,2})$ of the wrapped phase difference is almost as sharp as that of the clean data [Figs. 2(e) and 2(f) vs Fig. 2(b)]. The power spectra are also plotted for comparison. It shows that the subharmonics and subtle structures are buried by measurement noise [Fig. 2(g) vs Fig. 2(h)], while NPE and LP can recover most of them [Fig. 2(g) vs Fig. 2(i)]. If the narrow bandpass filter is applied to noisy data, then all the out-band structures will be removed.

The synchronization index $\rho=(S_{\max}-S)/S_{\max}$ is used to quantify the degree of phase synchronization in the coupled systems, where $S=-\Sigma_{i=1}^{K}P_i \ln P_i$ is the entropy of the distribution $P(\Delta\Psi_{1,2})$, $S_{\max}=\ln K$, and K is the number of bins of distribution [5,11]. It is reported that overembedding [30] (i.e., an embedding of excessively high dimension) may yield better result of noise reduction by LP [29]. For NPE and P-LP, an embedding of relatively higher dimension leads to a closer estimation of synchronization index to that calculated from clean data [Fig. 3(a)], and relatively more neighbors also yield a higher estimation of synchronization index [Fig. 3(b)]. For data with higher noise level, a few more neighbors may yield a little better results. For P-LP, simulation results also show that the synchronization index ρ decreases slowly (less than 6.2% for M from 3 to 10, when η=0.7) with respect to the increase of dimension M of the signal subspace space. Considering that the performances of the proposed schemes are not very sensitive to the values of parameters after they reach particular values, the parameters are simply set as follows: τ=1, d=80, N=20, and M=5, unless stated otherwise. More discussions on these parameters can be found in [21,27–29].

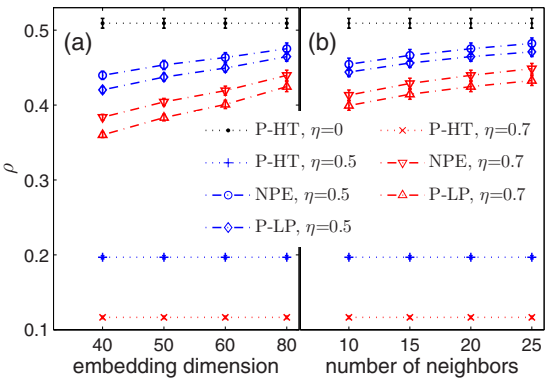

FIG. 3. (Color online) The estimated synchronization index ρ with respect to embedding dimension [(a), N=20] and the number of neighbors [(b), d=80] for synchronous Rössler systems (ε=0.035). Ten realizations of each case are calculated, and their means and standard deviations are plotted. The results (not included in this contribution for briefness) of similar simulations to the nonsynchronous Rössler systems (ε=0.01) show that ρ increases very slowly with the increase of the value of parameters d and N.

Figure 4 shows the results of the proposed schemes to data with different noise levels. For both the synchronous

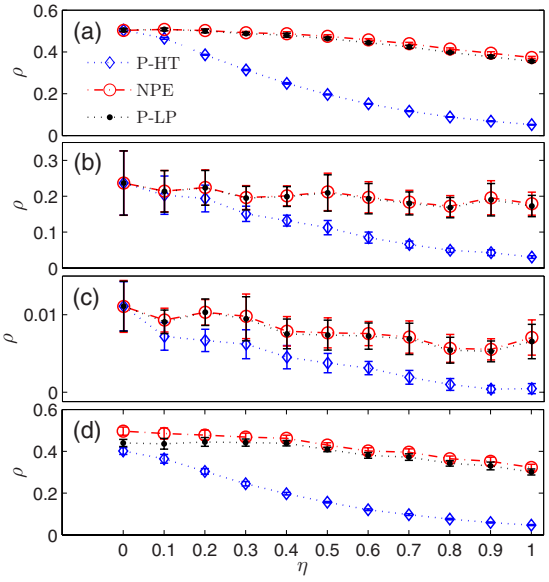

FIG. 4. (Color online) The estimated synchronization index ρ with respect to the level of measurement noise for the cases of synchronous [(a), ε=0.035], nearly synchronous [(b), ε=0.027], and nonsynchronous [(c), ε=0.01] states, which are with only measurement noise, and the case that is also with dynamic noise [(d), ε=0.2, $\sigma_{\zeta_{1,2}}$=0.1]. Ten realizations of each case are calculated.

[Fig. 4(a), $\varepsilon=0.035$] and the nearly synchronous [Fig. 4(b), $\varepsilon=0.027$] Rössler systems, the synchronization indexes estimated by P-HT descend quickly as the noise level increases, which may mislead that the coupled systems are nonsynchronous or weakly synchronous even though they are actually synchronous. The synchronization indexes estimated with the proposed schemes are more robust for noise, and are very close to that calculated from clean data ($\eta=0$), when the noise level is not so high [Fig. 4(a), $\eta<0.5$]. For the nonsynchronous systems [Fig. 4(c), $\varepsilon=0.01$], the synchronization indexes estimated by the proposed schemes are also close to that calculated from clean data. For these three cases, the proposed schemes do not yield overestimation of the degree of synchronization, and thus overcome the problem of overestimation that may arise from the linear bandpass filter [11]. Note that the coupling strength of these three cases are adopted from that used in [5].

Further, the proposed schemes are applied to data measured from coupled Rössler systems with dynamic noise. As Fig. 4(d) indicates, the synchronization indexes estimated by P-HT decrease quickly as the level of measurement noise increases. What is more, when the level of measurement noise is not so high ($\eta\leq 0.6$), the indexes are overestimated by NPE and P-LP, compared with the result of the case with no measurement noise ($\eta=0$) by P-HT. This is because the integrated data from systems with dynamic noise are not smooth and appear to be noisy even with no measurement noise. Both NPE and P-LP can reduce the effect of coarseness in data, and thus overestimate the degree of phase synchronization. The overestimation tends to fade off as the level of dynamic noise decreases. One way to deal with data with dynamic noise is the method of *shadowing* [31], which yields a smooth shadowing trajectory that is close to the coarse trajectory with dynamic noise. We conjecture that the synchronization index estimated by P-HT from the shadowing trajectory may be close to the indexes estimated by NPE or P-LP from the coarse data with only dynamic noise ($\eta=0$). Here, we do not discuss shadowing with more details because it is not the focus of this contribution.

For the data measured from noncoherent systems (e.g., the funnel Rössler systems), the phase definition with the Hilbert transform is not immediately applicable. One way to deal with this problem is to define the instantaneous phase based on the concept of curvature of an arbitrary curve [3,10]. For any two-dimensional curve $\mathcal{C}_1=(x,y)$ whose curvature is positive, the curve $\mathcal{C}_2=(\dot{x},\dot{y})$ cycles monotonically around a fixed point, and the phase can be always defined as

$$\phi=\arctan\frac{\dot{y}}{\dot{x}}. \tag{10}$$

The coupled funnel Rössler systems [Eq. (4), $\alpha=0.25$, $\beta=0.2$, $\gamma=10$, and $\sigma_{\xi_{1,2}}=0$] are studied with this phase definition. A smaller sampling interval $\Delta t=0.05$ is used, so that more smooth derivatives [Eq. (10)] can be obtained, and 40 000 samples are measured after the transient state. Data measured from variables $x_{1,2}$ and $y_{1,2}$ are all added with measurement noise, i.e., $s_{1,2}=x_{1,2}+\xi_{1,2}$ and $s_{3,4}=y_{1,2}+\xi_{3,4}$, where $\xi_{1,2}\sim N(0,\eta^2\sigma^2_{x_{1,2}})$, $\xi_{3,4}\sim N(0,\eta^2\sigma^2_{y_{3,4}})$, and η is the relative level of measurement noise. The LP method [$N=20$, $M=5$, $\tau=4$, and $d=80$, so that the length of the embedding window $(d-1)\tau\Delta t$ is almost equal to that used for the case of coherent Rössler systems] is applied to all the noisy data $\{s_{1,2,3,4}\}$ separately, yielding the estimation of $\{x_{1,2}\}$ and $\{y_{1,2}\}$, i.e., $\{\hat{x}_{1,2}\}$ and $\{\hat{y}_{1,2}\}$. Then the phases of systems (1, 2) are estimated via Eq. (10) with $\{\hat{x}_{1,2}\}$ and $\{\hat{y}_{1,2}\}$, respectively. Simulation results show that some degree of phase synchronization can be detected from data (actually synchronous) when the level of measurement noise is small ($\eta<0.1$). This is because the derivative [Eq. (10)] is very sensitive to noise. So the phase definition Eq. (10) seems not to be a robust measure for detecting phase synchronization in noisy data. One possible method is statistical measure of recurrences introduced recently [3]; but this method cannot indicate the degree of synchronization in local time.

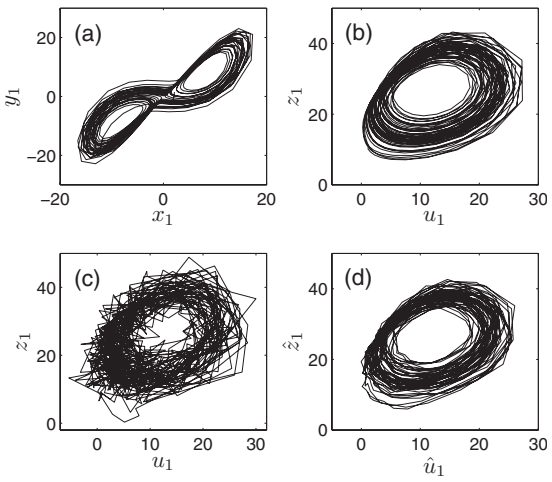

FIG. 5. Attractors of the Lorenz system reconstructed with (a) clean Lorenz data in the (x,y) plane, (b) clean Lorenz data ($\eta=0$) in the (u,z) plane, (c) noisy Lorenz data ($\eta=0.3$) in the (u,z) plane, and (d) the corresponding enhanced Lorenz data in the (u,z) plane, respectively.

B. Phase synchronization of coupled Lorenz systems

In this section, the LP method is applied as a preprocessing tool in detecting phase synchronization of the data from coupled Lorenz systems,

$$\dot{x}_{1,2}=10(y_{1,2}-x_{1,2})+\varepsilon(x_{2,1}-x_{1,2}),$$

$$\dot{y}_{1,2}=(r_{1,2}-z_{1,2})x_{1,2}-y_{1,2},$$

$$\dot{z}_{1,2}=x_{1,2}y_{1,2}-\frac{8}{3}z_{1,2}, \tag{11}$$

where $r_1=28$, $r_2=28.02$, and $\varepsilon=3.8$ is the coupling strength. Ten-thousand samples are measured with sampling interval $\Delta t=0.04$. In the (x,y) plane, the Lorenz attractor has two rotation centers [Fig. 5(a)], and the definition of phase with the Hilbert transform is not applicable. Considering the symmetry of Lorenz attractor, the phase of the Lorenz oscillator can be defined with its projection on the (u,z) plane,

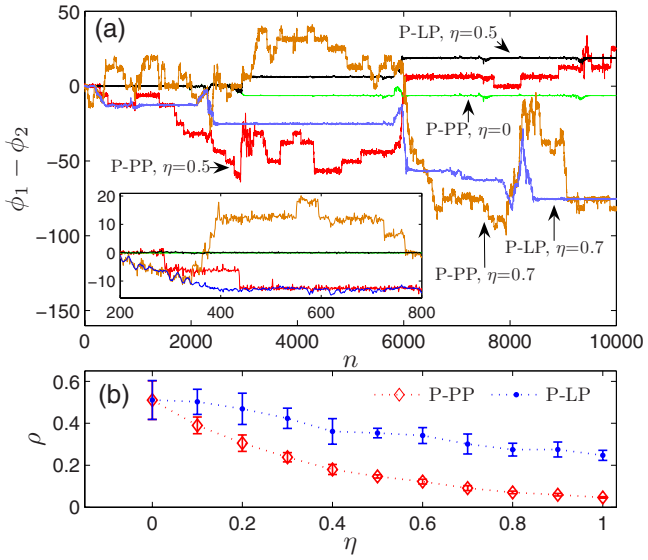

FIG. 6. (Color online) (a) The unwrapped phase difference of coupled Lorenz systems, and (b) their synchronization index ρ (ten realizations of each case) with respect to the level of measurement noise. P-PP denotes the results that the phase is defined in the projection plane [Eq. (12)] with no filtering to noisy data.

$$\phi = \arctan\frac{z - z_0}{u - u_0}, \tag{12}$$

where $u=\sqrt{x^2+y^2}$, $u_0=12$, and $z_0=27$ [9].

In the (u,z) plane, the attractor constructed with clean data [Fig. 5(b)] rotates around one center (u_0,z_0). Measurement noise, $\xi_{1,2}\sim N(0,\eta^2\sigma^2_{u_{1,2}})$, $\xi_{3,4}\sim N(0,\eta^2\sigma^2_{z_{1,2}})$, are added to $u_{1,2}$ and $z_{1,2}$, respectively. It can be observed that the attractor, distorted by noise [Fig. 5(c)], is almost recovered [Fig. 5(d)] after noise reduction by the LP method ($N=20$, $M=5$, $\tau=1$, and $d=80$). Note that the unwrapped phase difference fluctuates intensely [Fig. 6(a), "P-PP, $\eta=0.5$" and "P-PP, $\eta=0.7$"] due to measurement noise, though the systems are intrinsically synchronous [Fig. 6(a), "P-PP, $\eta=0$"]. However, these fluctuations can be greatly reduced by applying the LP method, resulting in long epoches of phase locking [Fig. 6(a), "P-LP, $\eta=0.5$" and "P-LP, $\eta=0.7$"]. Thus the degree of phase synchronization can be detected reliably from noisy data, which is more clearly demonstrated as the results summarized in Fig. 6(b).

In comparison with the LP method, the effect of bandpass filter in detecting phase synchronization is studied. The Gaussian envelop filter, introduced in [32], is applied to noisy data $u_{1,2}$ and $z_{1,2}$, respectively, and then the instantaneous phase is computed via Eq. (12) with the output of the filter. As Fig. 7 illustrates, this scheme, denoted as PBP, is sensitive to the band width (Δf) of the filter, and may overestimate the degree of synchronization even when the data is clean (P-PP, $\eta=0$).

IV. CONCLUSIONS AND DISCUSSIONS

Two schemes are proposed to detect phase synchronization from chaotic data contaminated by noise. One is the method of neighborhood-based phase estimation (NPE), the other adopts the local projection (LP) method as a preprocessing filter for noisy data. They are applied to data measured from two typical chaotic systems, i.e., the coupled Rössler systems and the coupled Lorenz systems. Simulation results show that the estimated instantaneous phase suffers much less from artificial phase slips caused by noise, and thus the degree of phase synchronization can be reliably detected even when the noise level is relatively high, avoiding the overestimation that may be introduced by the traditional linear bandpass filter. For the data with dynamic noise as well, overestimation may be introduced when the measurement noise level is not so high because the data measured from systems with dynamic noise are coarse even when there is no measurement noise. This overestimation tends to decrease as the level of dynamic noise decreases.

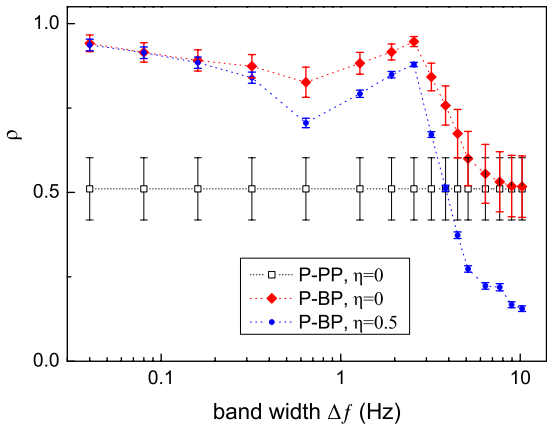

FIG. 7. (Color online) The synchronization index ρ (ten realizations of each case) with respect to the bandwidth Δf of the linear bandpass filter. The center frequency of the filter is set as 1.321 Hz, where the most energetic spectra of the Lorenz data are located around. Other details about the filter can be found in [32].

State recurrence is one important feature of chaotic systems. As discussed in the Introduction, it has been utilized in analyzing and processing various theoretical and experimental systems. Actually, nonlinear interdependence [14–16] and the statistical measure of recurrences [3] both utilize the idea of state recurrence defined by time delay embedding. Using the framework of localized sets [19], the typical events defined in those localized sets can also be considered as generalized "recurrences." The difference is that these "recurrences" are defined in a more general way (e.g., by the intersection of the trajectory with a local plane) rather than by the spatial nearness of vectors in the space reconstructed by time delay embedding.

Both schemes proposed in this contribution utilize the redundant information of state recurrences of chaotic data. The difference is that NPE estimates the instantaneous phase directly by averaging the analytical trajectories of neighbors, bridging time delay embedding to instantaneous phase estimation; while the scheme incorporating LP estimates the instantaneous phase from data after noise reduction. In the proposed schemes, the recurrences (i.e., neighbors) are defined

in the overembedded phase space (i.e., with long embedding window). Thus on the one hand, the recurrences collected from noisy data are more likely to be true recurrences (the recurrences collected form clean data are considered as true recurrences here); on the other hand, the proposed schemes may not be suitable for spiking and/or bursting neurons because spikes will dominate in collecting recurrences. It is difficult to design a method which is both robust to noise and applicable to various data. Usually, methods focus on just one point, the proposed schemes in this contribution focus on robustness.

ACKNOWLEDGMENT

This research was funded by Hong Kong University Grants Council Grant Competitive Earmarked Research Grant (CERG) No. PolyU 5269/06E.

[1] A. Pikovsky, M. Rosenblum, and J. Kurths, *Synchronization: A Universal Concept in Nonlinear Sciences* (Cambridge University Press, Cambridge, England, 2001).
[2] M. G. Rosenblum, A. S. Pikovsky, and J. Kurths, Phys. Rev. Lett. **76**, 1804 (1996).
[3] J. Kurths, M. C. Romano, M. Thiel, G. V. Osipov, M. V. Ivanchenko, I. Z. Kiss, and J. L. Hudson, Nonlinear Dyn. **44**, 135 (2006).
[4] D. J. DeShazer, R. Breban, E. Ott, and R. Roy, Phys. Rev. Lett. **87**, 044101 (2001).
[5] P. Tass, M. G. Rosenblum, J. Weule, J. Kurths, A. Pikovsky, J. Volkmann, A. Schnitzler, and H.-J. Freund, Phys. Rev. Lett. **81**, 3291 (1998).
[6] J. M. Hurtado, L. L. Rubchinsky, and K. A. Sigvardt, J. Neurophysiol. **91**, 1883 (2004).
[7] M. Le Van Quyen and A. Bragin, Trends Neurosci. **30**, 365 (2007).
[8] A. E. Hramov and A. A. Koronovskii, Chaos **14**, 603 (2004).
[9] A. S. Pikovsky, M. G. Rosenblum, G. V. Osipov, and J. Kurths, Physica D **104**, 219 (1997).
[10] J. Y. Chen, K. W. Wong, and J. W. Shuai, Phys. Lett. A **285**, 312 (2001).
[11] L. Xu, Z. Chen, K. Hu, H. E. Stanley, and P. C. Ivanov, Phys. Rev. E **73**, 065201(R) (2006).
[12] A. G. Rossberg, K. Bartholomé, and J. Timmer, Phys. Rev. E **69**, 016216 (2004).
[13] M. Palus, Phys. Lett. A **235**, 341 (1997).
[14] J. Arnhold, P. Grassberger, K. Lehnertz, and C. E. Elger, Physica D **134**, 419 (1999).
[15] X. Hu and V. Nenov, Phys. Rev. E **69**, 026206 (2004).
[16] M. A. Kramer, E. Edwards, M. Soltani, M. S. Berger, R. T. Knight, and A. J. Szeri, Phys. Rev. E **70**, 011914 (2004).
[17] R. Quian Quiroga, A. Kraskov, T. Kreuz, and P. Grassberger, Phys. Rev. E **65**, 041903 (2002).
[18] T. Kreuz, F. Mormann, R. G. Andrzejak, A. Kraskov, K. Lehnertz, and P. Grassberger, Physica D **225**, 29 (2007).
[19] T. Pereira, M. S. Baptista, and J. Kurths, Phys. Rev. E **75**, 026216 (2007).
[20] F. Takens, *Detecting Strange Attractors in Turbulence*, Springer Lecture Notes in Mathematics Vol. 898 (Springer, Berlin, 1981), pp. 366—381.
[21] J. Sun, Y. Zhao, T. Nakamura, and M. Small, Phys. Rev. E **76**, 016220 (2007).
[22] J. D. Farmer and J. J. Sidorowich, Phys. Rev. Lett. **59**, 845 (1987).
[23] J. B. Gao, Phys. Rev. Lett. **83**, 3178 (1999).
[24] R. Cawley and G.-H. Hsu, Phys. Rev. A **46**, 3057 (1992).
[25] H. Kantz, T. Schreiber, I. Hoffmann, T. Buzug, G. Pfister, L. G. Flepp, J. Simonet, R. Badii, and E. Brun, Phys. Rev. E **48**, 1529 (1993).
[26] J. Sun, Y. Zhao, J. Zhang, X. Luo, and M. Small, Phys. Rev. E **76**, 026211 (2007).
[27] H. Kantz and T. Schreiber, *Nonlinear Time Series Analysis*, 2nd ed. (Cambridge University Press, Cambridge, England, 2003).
[28] P. Grassberger, R. Hegger, H. Kantz, C. Schaffrath, and T. Schreiber, Chaos **3**, 127 (1993).
[29] J. Sun, N. Zheng, and X. Wang, Signal Process. **87**, 2431 (2007).
[30] R. Hegger, H. Kantz, L. Matassini, and T. Schreiber, Phys. Rev. Lett. **84**, 4092 (2000).
[31] J. D. Farmer and J. J. Sidorowich, Physica D **47**, 373 (1991).
[32] D. Vakman, IEEE Trans. Instrum. Meas. **43**, 668 (1994).